Available online at www.sciencedirect.com
SCIENCE DIRECT®
International Journal of Heat and Mass Transfer 48 (2005) 5179–5191
International Journal of HEAT and MASS TRANSFER
www.elsevier.com/locate/ijhmt

Mist/steam heat transfer of multiple rows of impinging jets

Ting Wang [a,*], J. Leo Gaddis [b], Xianchang Li [a]

[a] Energy Conversion and Conservation Center, University of New Orleans, New Orleans, LA 70148-2220, United States
[b] Department of Mechanical Engineering, Clemson University, Clemson, SC 29634-0921, United States

Received 18 June 2004; received in revised form 30 July 2005
Available online 14 October 2005

Abstract

Internal mist/steam blade cooling technology is considered for future high-temperature gas turbine systems that burn hydrogen or synthetic gases. This paper experimentally investigates the mist/steam heat transfer of three rows of circular jet impingement in a confined channel. Experiments were conducted with Reynolds numbers at 7500 and 15,000 and heat fluxes ranging from 3350 to 13,400 W/m^2. The results indicate that the wall temperature significantly decreased because of mist injection. The cooling enhancement region of the three-row jet impingement jets is more extensive than those employing one row of circular jets or a slot jet. The highest enhanced region spans about five jet diameters and becomes negligible downstream. The maximum local enhancement is up to 800% by injecting 3.5% of mist at low heat flux condition and 150% at high heat flux condition. The average cooling enhancement can achieve more than 100% within two jet-diameter distance from the stagnation line at $Re = 15{,}000$ and $m_l/m_s = 1.5\%$.

Keywords: Jet impingement; Mist/steam cooling; Two-phase flow heat transfer; Turbine blade cooling

1. Introduction

Due to its high heat and mass transfer rate, single-phase jet impingement has been used in many industrial fields such as annealing of metal and plastic sheets and cooling of electronic components, etc. Published data also show that the addition of mist to an air or steam flow can enhance heat transfer significantly [1–6]. It has been recognized that mist/steam jet impingement could be an excellent candidate for enhancing gas turbine heat transfer. The inlet temperature of advanced gas turbines is continuously increasing to achieve a higher overall efficiency. Therefore, gas turbine engines are usually designed to operate at temperatures much higher than the allowable metal temperature of the airfoils. This trend will continue especially when future gas turbines are required to burn hydrogen or synthetic gases, which have higher flame temperatures than natural gas. It is essential that innovative methods be explored and investigated to provide significant cooling enhancement than the existing methods for protecting the airfoils as well as other hot parts from metallurgical failures. Mist/steam cooling can provide such a role. Compared to traditional gas turbine cooling technology such as air film cooling, mist/steam cooling brings an extra advantage, with significant enhancement of cooling effectiveness, less pressure drop, significant reduction of cooling air, and reduction of temperature drop

* Corresponding author. Tel.: +1 504 280 7183; fax: +1 504 280 5539.
E-mail addresses: twang@uno.edu (T. Wang), leo.gaddis@ces.clemson.edu (J.L. Gaddis), xli8@uno.edu (X. Li).

0017-9310/$ - see front matter © 2005 Elsevier Ltd. All rights reserved.
doi:10.1016/j.ijheatmasstransfer.2005.07.016

Nomenclature

B	width of heat element
d	diameter of jets
d_{10}	arithmetic mean diameter of droplets
d_{30}	volume mean diameter of droplets
d_{32}	Sauter mean diameter of droplets
h	heat transfer coefficient
I	current through the heater
k	heat conductivity
m	mass flow rate
Nu	Nusselt number (hd/k_s)
q''	heat flux
Re	Reynolds number ($\rho_s V_j d/\mu_s$)
T	temperature
V_j	average jet velocity at jet exit
x	coordinate along the target wall

Greek symbols

δ	thickness of heater elements
μ	dynamic viscosity
ρ	density
ξ	resistivity (Ω m)

Subscripts

0	stagnation point or single-phase steam
j	jet
l	liquid phase
s	steam
w	wall

between combustor and turbine inlet temperature, etc. See detailed discussion in [1].

Basically, the mechanism of heat transfer enhancement by using mist/steam flow can be summarized as follows: (a) the latent heat of evaporation serves as a heat sink to absorb large amounts of heat; (b) the heat sink effect reduces the bulk temperature and increases the temperature gradient near the wall, which further increases heat conduction from the wall; (c) the direct contact of a small amount of liquid droplets with the wall further increases heat transfer via direct wall-to-liquid heat conduction and results in accelerated evaporation; (d) the propulsive momentum induced by wall-to-liquid droplet vaporization accelerates the transport of energy from the wall to the core flow; (e) steam and water have higher specific heat capacity (C_p) than air; (f) the flow mixing is increased by steam–particle interactions through particle dynamics, including forces such as Saffman force and evaporation force. Among these effects, it has been found that the direct droplet deposit and evaporation play a dominant role [7].

Not many studies have been found on the two-phase impingement heat transfer, especially on steam flow with droplets. Note that spray cooling is different from mist cooling. Spray cooling usually involves large liquid droplets moving with high-inertia streams instead of passive droplets that are transported by a flow medium such as mist in a steam flow. Below is a brief review of references related to cooling by mist/steam flow or impinging jets.

Goodyer and Waterston [8] studied the possibility of using mist/air impingement for turbine blade cooling. The surface temperature in their study was above 600 °C. They suggested that the heat transfer was dominated by partial contact between the droplets and the target surface during which the droplets vaporized at least partially. A vapor cushion and the elastic deformation of the droplets may reject the droplets from the heated surface. Heat transfer at the stagnation point can be enhanced by 100% with an addition of 6% water. The droplet size ranged from 30 to 200 μm, which has little effect on heat transfer.

By studying the mist/air heat transfer in a vertical rectangular tube heated on one side, Takagi and Ogasawara [9] identified a post-dryout region within which the heat transfer coefficient increased with droplet concentration and flow velocity but decreased when the droplet size increased. If the wall was wet, which occurred at lower wall temperature, the heat transfer coefficient increased with increased heat flux.

Ganic and Rohsenow [10] studied gas flow heat transfer with water droplets. They demonstrated that the total heat transfer flux is the sum of a single-phase component, and a component due to direct impact of the droplets. When the droplets moved inside the thermal boundary layer, they were subjected to an extra lift force that is caused by an imbalanced evaporation rate. The droplets tend to move away from the higher temperature region, which is the heated surface in a cooling application. Mastanaiah and Ganic [11] reported the experimental results on mist/air in the post-dryout region inside a vertical circular tube. They confirmed the heat transfer coefficient decreased with increased wall temperature, which means the relative contribution of the dispersed droplets decreased.

The pure effect of particles on flow turbulence structure was examined in the study of Yoshida et al. [12], which was conducted on air jets with a suspension of 50-μm glass beads. Results indicated that the gas velocity decreased due to the rebound of beads in the impinging jet region, but the velocity fluctuation in the normal direction increased. The heat transfer coefficient could

be 170% higher than the single-phase flow when the mass flow ratios (solid/gas) reached 0.8. It was also found that the effect was slight in the wall–jet region, i.e., downstream of the impingement area.

To explore an innovative approach to cool future high-temperature gas turbines, the authors' research group conducted a series of studies on mist/steam cooling. Guo et al. [1,2] studied the mist/steam flow and heat transfer in a highly heated straight tube. Measured with a Phase Doppler Particle Analyzer (PDPA) system, the droplet size ranged from 2 to 12 μm. The highest local heat transfer enhancement of 200% was achieved with 5% mist, and the average enhancement was 100%. In [3], mist/steam cooling was studied by the same experimental facility in a highly heated, horizontal 180° tube bend. The overall cooling enhancement of the mist/steam flow ranged from 40% to 300% with maximum local cooling enhancement being over 800%, which occurred at about 45° downstream of the inlet of the test section. Li et al. [4] reported results of mist/steam cooling with a slot jet on a heated flat surface. It was found that stagnation point heat transfer could be enhanced over 200% by adding 1.5% mist (in mass) to the steam flow. The mist enhancement declined to near zero by five slot widths downstream. Li et al. [5] presented the results of a row of discrete jets. The results showed that the discrete jets achieve higher cooling effectiveness in steam-only flow but produced lower cooling enhancement in mist/steam flow when compared to slot jet. Experiments conducted in [6] show the cooling effect of a mist/steam slot jet impinging on a concave surface. Enhancements of 30–200% at the stagnation point were obtained with an addition of mist 0.5% or less by mass. The cooling enhancement is greater at lower heat flux as has been observed in other studies.

This paper presents a continuous experimental study on mist/steam cooling with three rows of circular jet impingement. A region of high cooling enhancement is observed and is more extensive than those employing one row of circular jets or slot jet.

2. Experimental facility

2.1. Experimental system

As shown in Fig. 1, the experimental system implements the following functionals. Water is atomized into

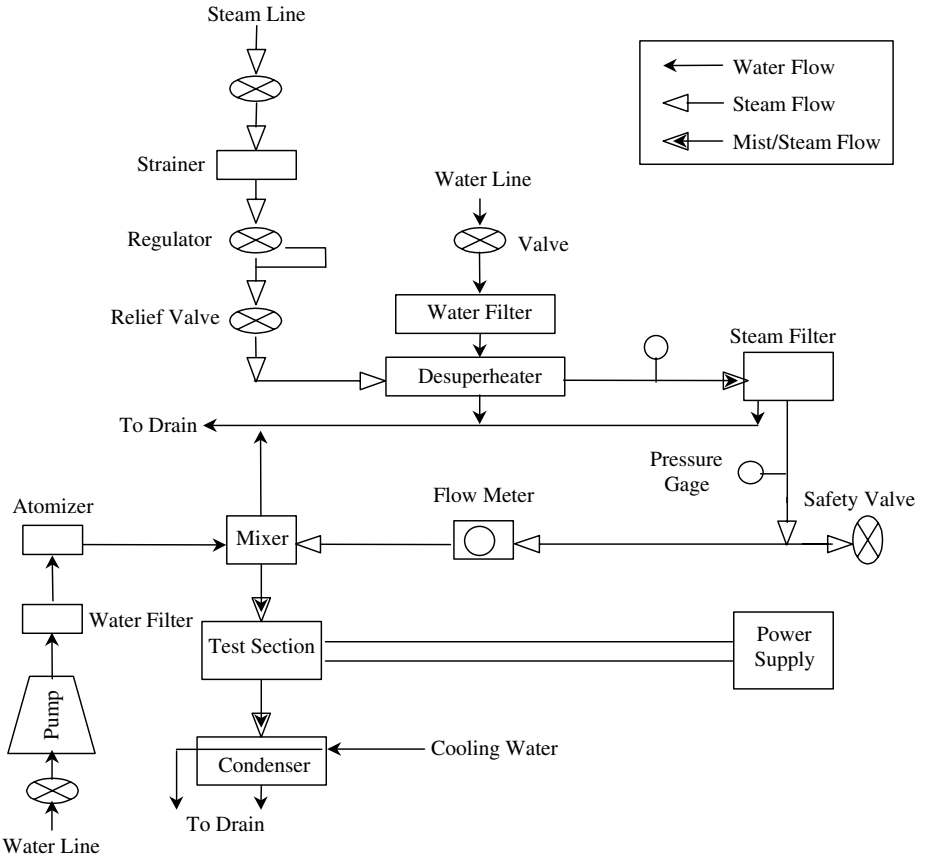

Fig. 1. Schematic of the experimental system.

droplets through atomizers (Mee Industries Inc.) and a high-pressure pump (68 bar). The steam flow first comes from the existing steam system in the building, and then passes through a strainer, a regulatory system, a desuperheater, and a filter tube that supplies a clean and dry saturated steam to mix with the droplets in a mixing chamber. The mist/steam flow enters into the test section through a flexible silicon tube at a saturation pressure of about 1.2 bar at 103–104 °C. The exhausted mist/steam condenses into water in a condenser before being expelled.

Fig. 2a shows the schematic of the test section, which has the identical structure as in [4] except the injection plate. Fig. 2b shows the test section during installation. An optical window made of Pyrex constitutes part of the front wall. This Pyrex window allows laser beams to pass through so optical measurement can be conducted. The target surface consists of five discrete heater elements that cover the most interesting area. The segmented heated surface is mounted firmly to a backup plate of high temperature and low thermal conductivity. The middle one, which covers the stagnation point, is

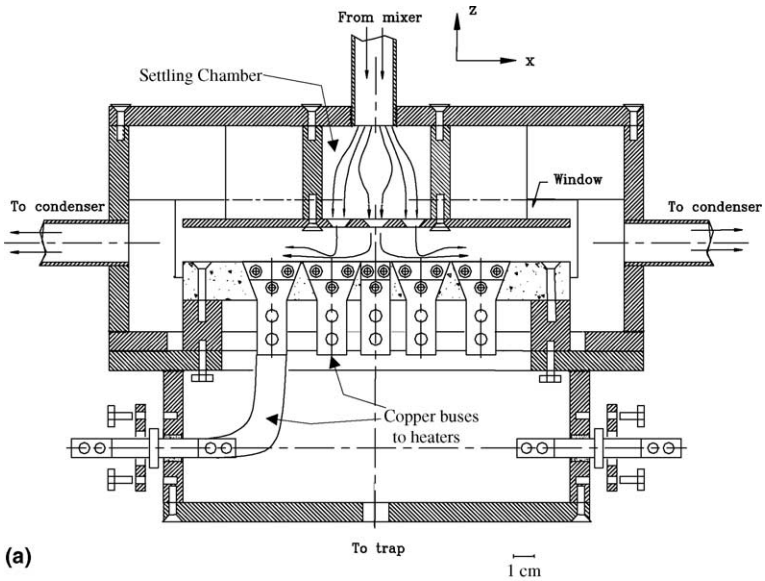

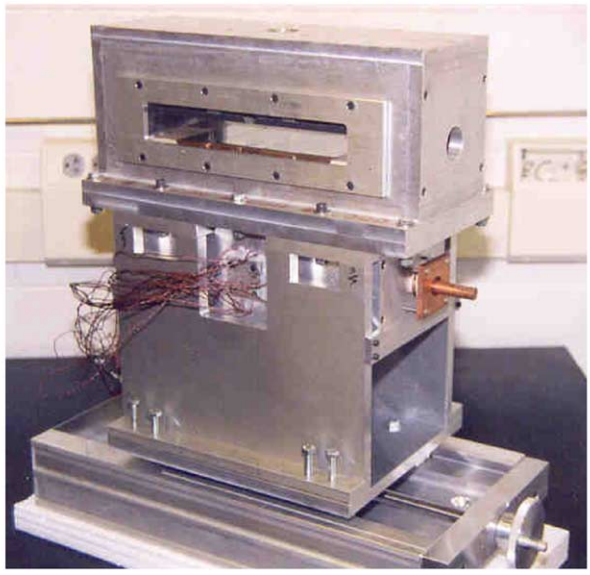

Fig. 2. Test section: (a) schematic and (b) before assembly.

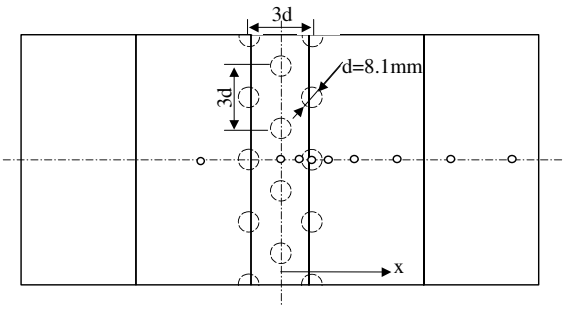

Fig. 3. Three rows, 12-hole jet plate.

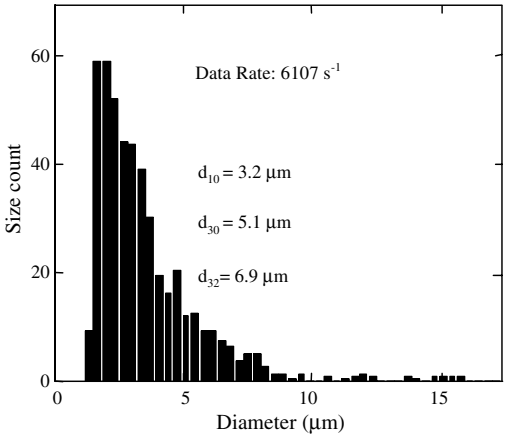

Fig. 4. Droplet size distribution.

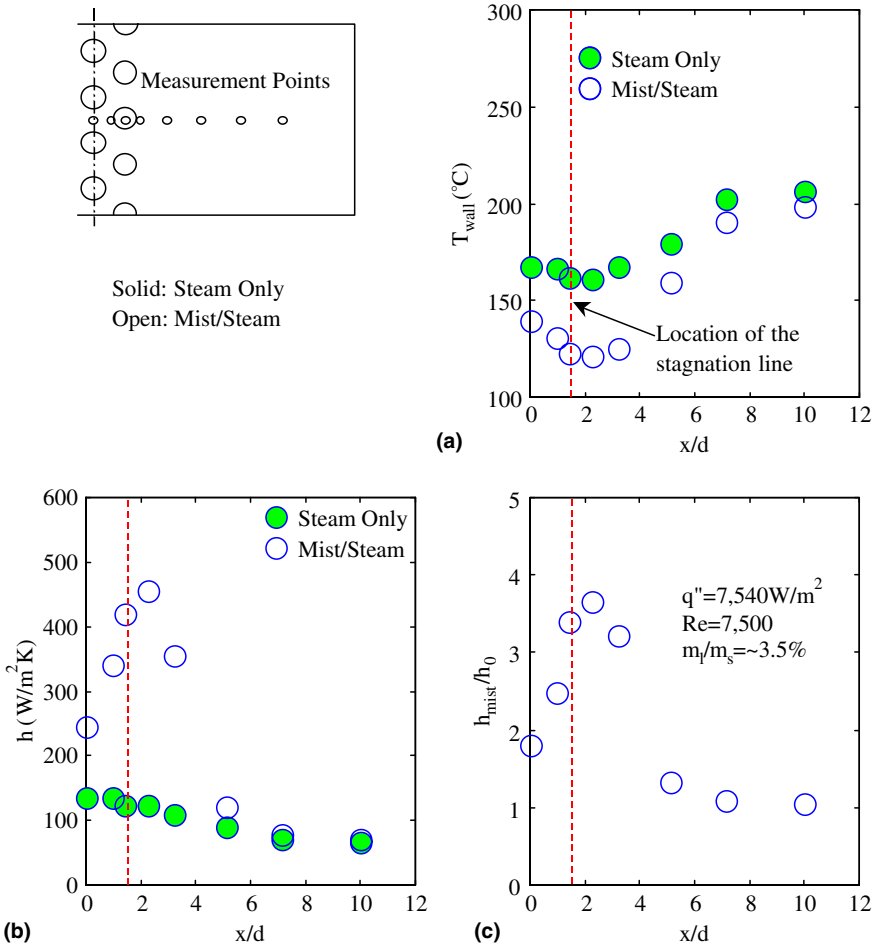

Fig. 5. Heat transfer results for 12 round mist/steam jets ($q'' = 7.54$ kW/m^2, $Re = 7500$ and $m_l/m_s = \sim 3.5\%$). (a) Wall temperature, (b) heat transfer coefficient and (c) ratio of heat transfer coefficient (enhancement).

only half the width of the other four identical elements (38×76 mm). The heater elements are directly heated by a DC power supply with high current (up to 750 A) and low voltage (0–7 V). Thermocouples are buried under the heater elements and are separated by a thin mica sheet.

Fig. 3 shows the injection geometry for the 12-hole tests as viewed from the injection plate. The holes and pattern for the central four holes are identical with the four-hole tests in [5]. The jet diameter is approximately 8.1 mm and uniform jet spacing of $3d$ is used. At equal Reynolds number, this device has three times the flow rate as the single row, four-hole device previously employed. The jet surface plate is spaced 22.5 mm from the heated section.

2.2. Experimental measurement and uncertainty analysis

Temperatures are measured by Omega 30-gage (about 0.25 mm in wire diameter) Chromel–Alumel (K type) thermocouples with braided fiberglass insulation. A data logger (FLUKE Model 2250) is used to monitor and record the temperature. The thermocouples, along with the data logger, were calibrated against a standard Resistance Temperature Device (RTD) system for nominal temperature uncertainty of 0.3 °C. As shown in Fig. 3, thermocouples are strategically placed at the centerline of the target wall and at about 1, 1.5, 2, 3, 5, 7 and 10 jet diameters away from the centerline. The temperature at the test section inlet and the temperature of the water used for the atomizer are also measured.

Steam flow rate is measured by an orifice flow meter. The catch-and-weigh method is also used to measure flow rates and to calibrate the flow meter in situ. Water flow from the trap under the mixer is essential for determining water concentration in the mist. The water flow rates from the traps just before the test section and at the bottom of the test section are also measured. The water flow rate to the atomizer can be adjusted by changing the pump pressure. Pressure gages before and after the steam filter measure the steam pressure.

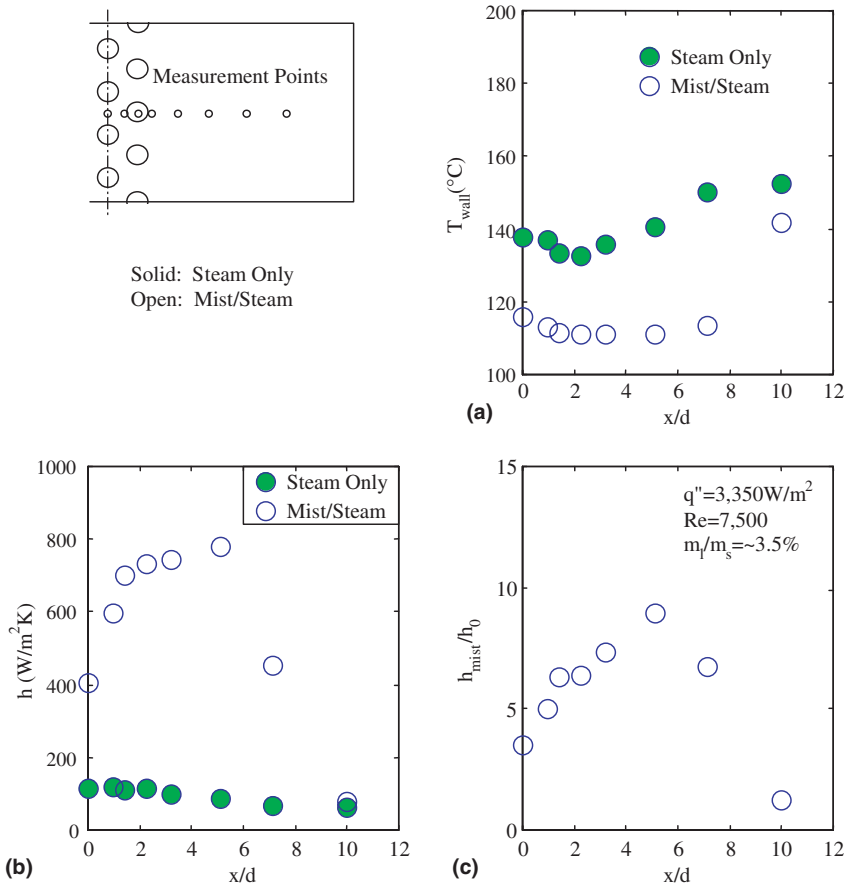

Fig. 6. Heat transfer results for 12 round mist/steam jets ($q'' = 3.35$ kW/m^2, $Re = 7500$ and $m_l/m_s = \sim 3.5\%$). (a) Wall temperature, (b) heat transfer coefficient and (c) ratio of heat transfer coefficient (enhancement).

The heater is heated with Joule heating. The current passed through the heater elements is given by the voltage across the precision shunt (with a resistance of $1.333 \times 10^{-4}\ \Omega$) of the power supply. The voltage across the test section is measured directly by a voltmeter. The heat flux on the heater can be obtained from the heating power divided by the heating area, assuming the heater has a uniform thickness. In this study, the heating power is directly obtained from the electrical resistance of the heater components and the current as follows:

$$q'' = I^2\xi/\delta B^2 \tag{1}$$

where I is the current and ξ is the resistivity of the heater materials. δ and B are the heater thickness and width, respectively. Calculation by this equation can avoid measurement error of the heater length and of the voltage across the test section due to contact resistance. The back heat loss, less than 5%, is corrected with a simple 1-D heat conduction model.

As in other studies, the heat transfer coefficient is obtained by

$$h(x) = \frac{q''(x)}{T_w(x) - T_j} \tag{2}$$

where q'' is the wall heat flux, T_w is the local wall temperature, and T_j is the temperature of the jet, which is nominally at 103 °C, measured by two thermocouples. The steam saturation temperature is taken as the jet temperature. The wall temperatures are read from the thermocouple measurements. Since the temperature drop across the heater is less than 0.5 °C, which is negligible compared with $(T_w - T_j)$, the reading of the thermocouples is directly used as the wall temperature.

The droplet size and velocity are measured with a Phase Doppler Particle Analyzer (PDPA) through the Pyrex windows. Fig. 4 shows a typical distribution of the droplets close to the stagnation point. The droplet size ranges from 1 to 15 μm with an arithmetic mean diameter (d_{10}) of 3.2 μm and a volume mean diameter (d_{30}) of 5.1 μm. The Sauter mean diameter (d_{32}) of this distribution is 6.9 μm. It can be seen that most of droplets are smaller than 5 μm.

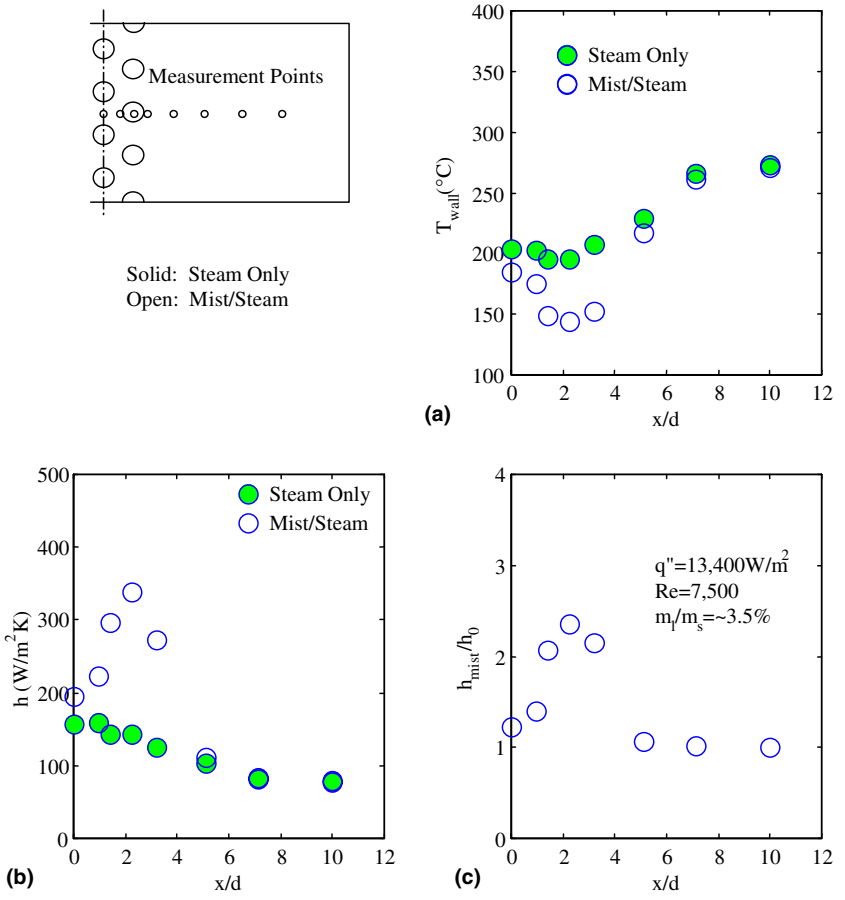

Fig. 7. Heat transfer results for 12 round mist/steam jets ($q'' = 13.4$ kW/m^2, $Re = 7500$ and $m_l/m_s = \sim 3.5\%$). (a) Wall temperature, (b) heat transfer coefficient and (c) ratio of heat transfer coefficient (enhancement).

An Nth-order uncertainty analysis is conducted in this study, based on the methodology developed by Moffat [13] and Wang and Simon [14]. The detailed analysis is documented in [15]. The uncertainty for heat transfer coefficient is about 5–7%, and the largest source is the heating voltage of the power supply. As to the flow rate, although the uncertainty for the steam flow is very small, the mist concentration has a large uncertainty (~40%) with the largest source of uncertainty coming from the sampling time. The main sources for the uncertainty of Reynolds number (1.65%) are the steam viscosity, μ_s, and the slot length.

3. Experimental results and discussions

Experiments were started with low Reynolds number and medium heat flux. As a baseline, Fig. 5 shows the heat transfer result of the 12 circular mist/steam jets at $q'' = 7540\ \mathrm{W/m^2}$, $Re = 7500$ and $m_l/m_s = 3.5\%$. Similar to the previous single-row results, the wall temperature decreases dramatically due to the addition of liquid droplets to steam flow, which results in significant heat transfer enhancement. Located downstream close to the stagnation point, the maximum enhancement is more than 250%. (The enhancement in this paper is defined as the ratio of heat transfer coefficient with and without mist minus one, $h_{mist}/h_0 - 1$.) It is believed that the flow structure pushes the maximum enhancement downstream. (The dashed line in the figure shows the stagnation line of the second row.) The enhanced region is extended to $x/d = 4$–5. Part of the reason for this extension is undoubtedly the additional row of holes. Another is possibly secondary flows generated in the downstream region. It is interesting to note that the enhancement on the centerline of the target wall is also notable almost 100% in this case.

After obtaining the baseline case, heat flux was decreased first and then increased to examine its effect on the enhancement. Figs. 6 and 7 show the cases with different heat fluxes. The maximum enhancement is about 800% when the heat flux drops to 3350 $\mathrm{W/m^2}$ while it

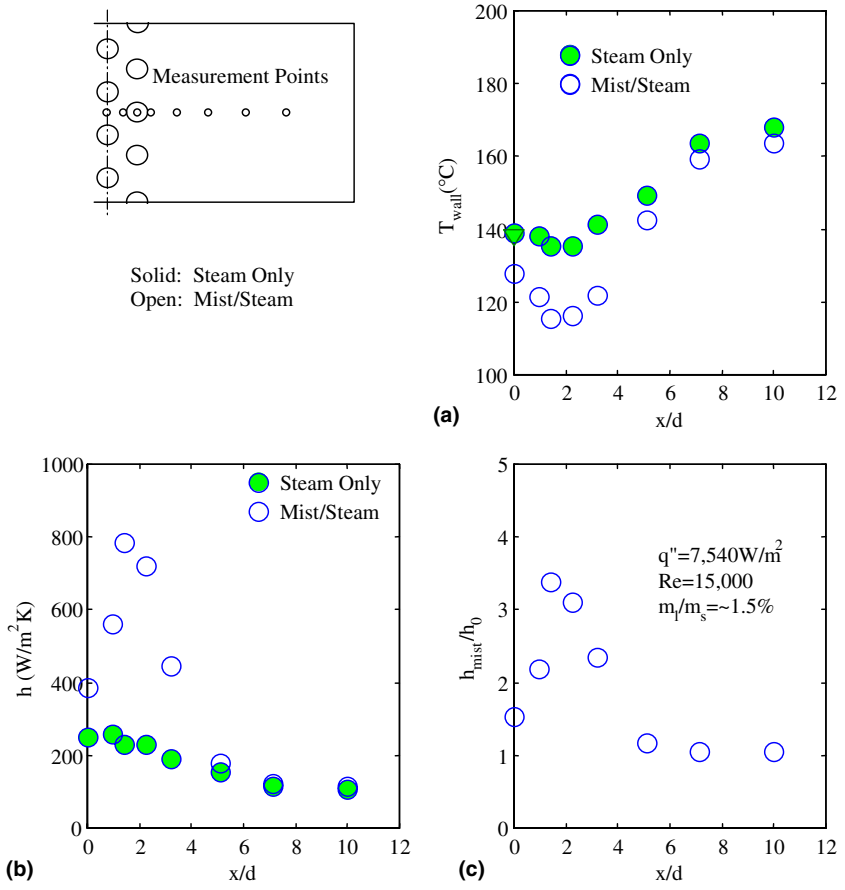

Fig. 8. Heat transfer results for 12 round mist/steam jets ($q'' = 7.54\ \mathrm{kW/m^2}$, $Re = 15{,}000$ and $m_l/m_s = \sim 1.5\%$). (a) Wall temperature, (b) heat transfer coefficient and (c) ratio of heat transfer coefficient (enhancement).

reduces to 150% at 13,400 W/m^2. This trend of reduced cooling enhancement with increased heat flux is consistent with those of previous experiments. This phenomenon can be interpreted as the enhancement from mist is dominated by direct evaporation of mist on the heated surface. Furthermore, the region of cooling enhancement also decreases in size with the increase of heat flux. The enhanced region is about 4d at high heat flux and is extended to 9d at low heat flux.

Experiments were also conducted at higher Reynolds number ($Re = 15{,}000$ at 1.5% mist) as shown in Figs. 8 and 9. In general, as little as 1.5% mist is capable of providing up to 250% or more cooling enhancement near stagnation region at the worst observed conditions. The average cooling enhancement can achieve 100% within 2d distance from the stagnation line. This powerful effect summarizes the potency of the mist cooling for situations having a direct impact on the heated surface. Farther downstream, the effect wanes, and location depends on flow conditions. For example, the effect wanes at $x = 6d$ when the Reynolds number is 15,000 and heat flux is 13.4 kW/m^2. The details of this waning effect are highly dependent on the conditions of the experiment.

Figs. 7 and 9 can be used to explore the effect of flow rate on mist/steam heat transfer. When Reynolds number increases, the mist concentration also changed due to the facility constraint. It can be seen that the increased flow velocity brings more droplets to the target surface, and that results in a considerable enhancement even with lower mist concentration. The higher cooling enhancement in Fig. 9 is also partially contributed by lower wall superheat. Note that although at a lower wall heat flux, comparison between Figs. 5 and 8 does not show an enhancement when flow rate is increased, it is believed that the cooling enhancement could be realized if the case in Fig. 8 would have been conducted using the higher mist concentration 3.5% as in the case in Fig. 5. Because of the strong impinging flow in Figs. 7–9, the maximum cooling enhancement tends to be close to the stagnation point. However, the overall region of enhanced cooling is reduced. From these results, it can be reasoned that the highest and most effective cooling enhancement is restricted to the region where direct

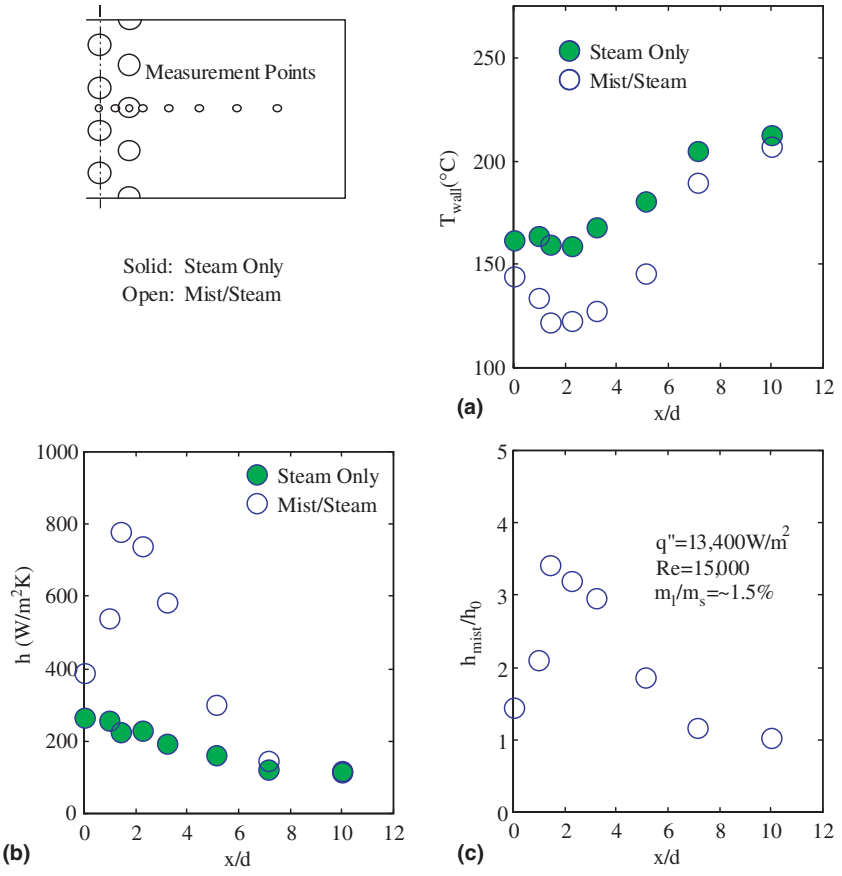

Fig. 9. Heat transfer results for 12 round mist/steam jets ($q'' = 13.4$ kW/m^2, $Re = 15{,}000$ and $m_l/m_s = \sim 1.5\%$). (a) Wall temperature, (b) heat transfer coefficient and (c) ratio of heat transfer coefficient (enhancement).

impact of droplets is most likely. There is almost certainly a spreading of the droplet impact pattern and some rebounding and second impact of droplets as predicted by CFD in the slot jet study [5]. The effect of increased mist concentration on cooling enhancement is not clearly seen in the present study although it is apparent that more mist will result in more cooling enhancement.

To examine the experimental data effectively, the results are summarized in Nusselt number as shown in Fig. 10. For the single-phase steam-only flow with a fixed Reynolds number, the Nusselt numbers collapse within 5% under different heat loads. However, the Nusselt number results for mist/steam flow vary significantly with mist concentrations and heat flux. The overall trend of mist enhancement to heat transfer can be concluded as above through Nusselt number analysis.

Detailed mist/steam heat transfer mechanisms were investigated and analyzed by Li et al. [7], in which the overall heat transfer of mist/steam is divided into three parts: heat transfer from the target wall to the steam flow (q_1''), heat transfer between steam and droplets (quenching effect, q_2''), and heat transfer from wall to droplets (q_3'). Therefore, the enhancement ratio can be given as

$$\frac{h_{\text{mist}}}{h_0} = \frac{q_1'' + q_2'' + q_3''}{q_1''} \tag{3}$$

The value of q_1'' can be evaluated by using the convective heat transfer coefficient of single-phase flow (h_0) and the temperature difference between the heated surface and steam flow. To evaluate q_2'', droplets are considered as a continuously distributed heat sink. The droplets evaporate into the superheated steam inside the thermal boundary layer and then quench the boundary layer. By solving the energy equation of the boundary layer, the change of the temperature distribution due to the droplet evaporation can be obtained. The higher temperature gradient near the heated surface represents the enhancement due to the quenching effect. Heat transfer from wall to droplets (q_3'') is considered through heat conduction when the droplets hit the surface. The value of q_3'' can be evaluated by calculating how many droplets will hit the wall at each location and how much thermal energy is transferred from the heated wall to the droplets. The droplet trajectories are tracked numerically to evaluate the intensity of the droplets hitting the wall. For any single droplet, a quasi-transient process is used to obtain the heat transfer between droplet and wall by assuming the droplet will hit, stay and bounce away from the wall after a certain superheat is reached. The heat transfer between an individual droplet and wall is eventually related to the surface superheat, droplet diameter, impact velocity, and droplet surface tension. The comprehensive modeling and evaluations of q_1'', q_2'', and q_3'' can be found in [7].

Depending on the mist flow conditions, heat conduction between the droplets and heated surface (q_3'') and the subsequent liquid evaporation contribute about 80–99% to the total enhancement ($q_2'' + q_3''$). One example from [7] shows $q_1'' = 3000\ \text{W/m}^2$, $q_2'' = 131\ \text{W/m}^2$, and $q_3'' = 4143\ \text{W/m}^2$. It is believed that the droplets only contact the wall for a very short time (residence time), which depends on the droplet size and wall temperature. The residence time of the droplets becomes less when the wall temperature increases due to the stronger heat conduction and faster water evaporation. Therefore, the total heat transfer between the droplets and wall is less dependent of the wall temperature as the wall heat flux increases. On the other hand, for the single-phase flow, the heat transfer is proportional to the temperature difference.

$$q_1'' = h_0(T_w - T_s) \tag{4}$$

Therefore, the enhancement ratio decreases as the heat flux (the wall temperature) increases. After the droplet impinging on the wall, the vapor expands almost 1000

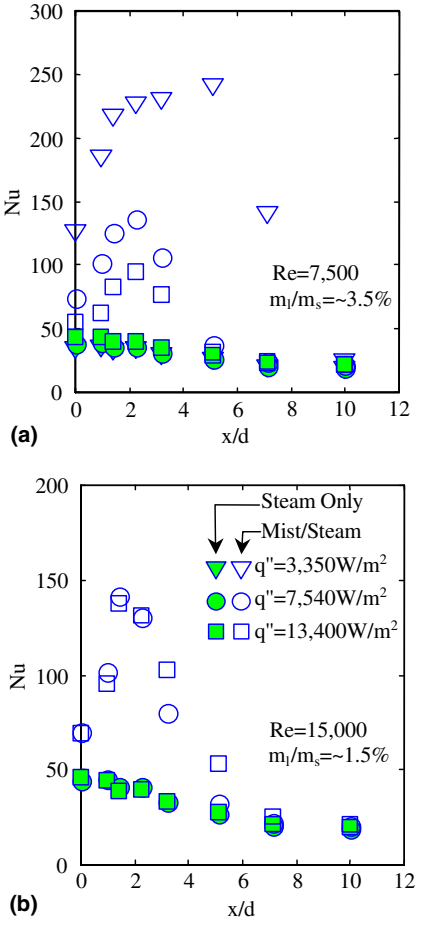

Fig. 10. Heat transfer results in Nusselt number. (a) $Re = 7500$ and (b) $Re = 15{,}000$.

times in volume from the liquid state. This quick expansion of vapor layer exerts a strong propulsive force, which propels the droplets from the wall. This is different from the film boiling stage of a typical pool/convective boiling phenomenon, in which the vapor film cannot escape from the surface and results in an insulation effect.

3.1. Comparison of heat transfer performance with previous cases

A comparison is made by examining the differences between single-row jets and three-row jets. Both enhancements are shown in Fig. 11 at different conditions. Note that the stagnation line of single-row jets is artificially moved to the same location as the three-row jets, which makes the comparison easier. From the two cases with different heat fluxes ($q'' = 3.35$ kW/m^2 and 7.54 kW/m^2) at low Reynolds number ($Re = 7500$) and high mist concentration ($m_l/m_s = \sim 3.5\%$), it can be seen that the enhancement for three-row jets is higher and more extended than that for one-row jets. Again, the strong interaction between jets and secondary flow contribute this difference. As the jet flow becomes stronger ($Re = 15{,}000$) and the mist concentration becomes lower ($m_l/m_s = \sim 1.5\%$), the enhancements of both one-row and three-row jets are similar. Although individual jets show no large difference, the overall region of enhanced cooling is definitely larger when multiple-row jets are used. For example, at $Re = 7500$, $q'' = 7.54$ kW/m^2, and $m_l/m_s = \sim 3.5\%$, the enhanced region of three-row jets is about 5d, compared to 2d for single-row jets.

Efforts were also made to compare the cooling performance of a single slot jet and three-row circular jets based on the same Reynolds number (Fig. 12). For the slot jet, the Reynolds number is defined using the hydraulic diameter as the length scale, which equals twice of the slot width "b". Fig. 12 shows that at a low heat flux rate (3350 W/m^2), the three-row mist/steam jets produce a higher heat transfer enhancement with more extended surface area than the slot jet. As the heat flux increases (Fig. 12b) or Reynolds number increases (Fig. 12c), the area of effective cooling enhancement becomes similar, but the three-row jets produce 30% higher cooling enhancement than the slot jet. It should be noted that at a given Reynolds number, the average velocity of the circular jets is about 1.85 times

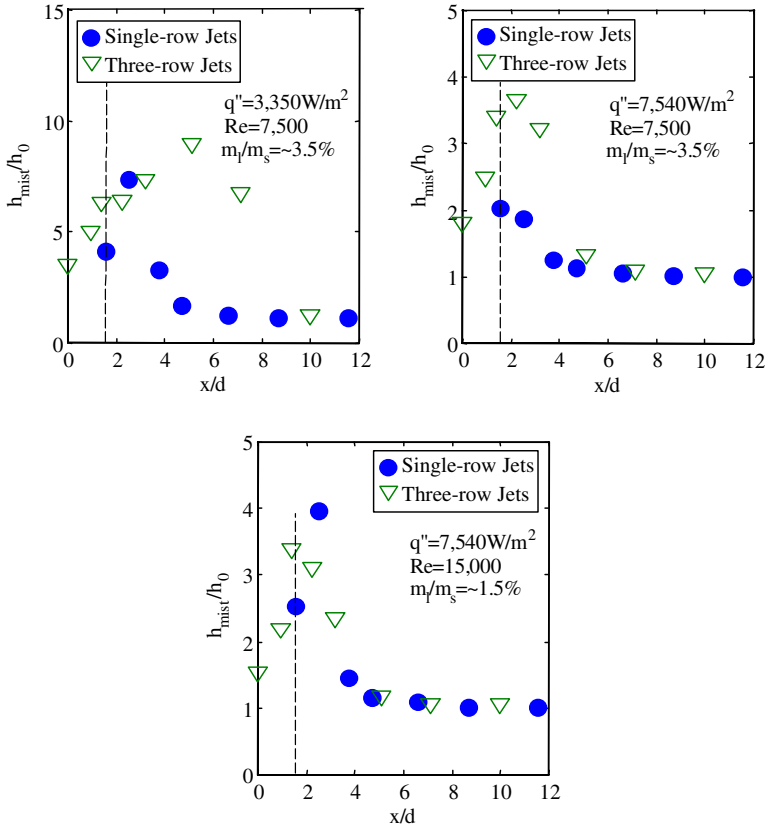

Fig. 11. Comparison of heat transfer enhancement for single-row and three-row round mist/steam jets.

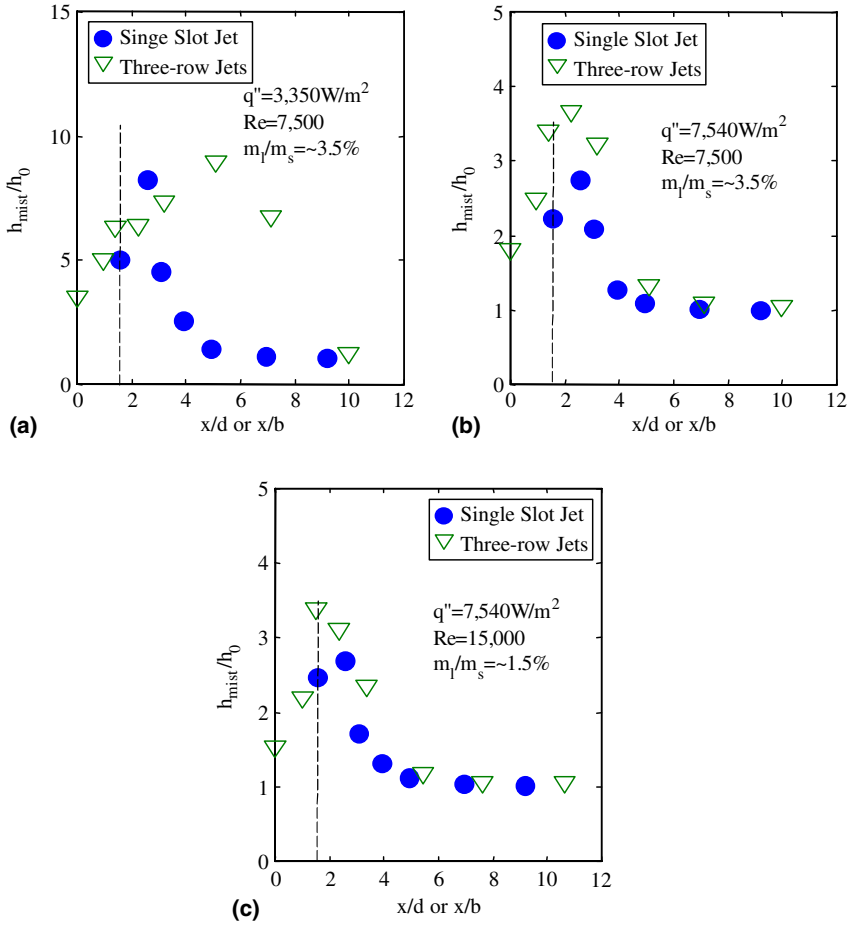

Fig. 12. Comparison of mist cooling enhancement for a single slot jet and three-row round jets.

that of a slot jet, which means stronger droplet impacts onto the wall.

The above comparisons are based on the same Reynolds number but at different mass flow rates for each scheme. Therefore, it is interested to use alternate criteria to make comparisons. One option is to compare the cooling effectiveness based on total thermal energy removed from the heated surface per mass flow rate, and another is to consider the cooling enhancement per unit surface area. Applying both criteria, the following analysis is made to provide an alternative way for comparison. At a fixed Reynolds number, the total steam mass flow rate of 12 circular jets is about 150% of the slot jet. Considering only the significant enhanced area (3*d* and 3*b*), the heat transfer coefficient of the three-row jets is about 1.25 times larger than the slot jet. The enhanced area of the three-row circular jets is about 25% larger than the slot jet for higher heat flux cases (Fig. 12b and c); therefore, it can be shown that the heat removal of the three-row jets, per mass flow rate, per unit surface area will be about the same as the slot jet.

3.2. Projection to prototype scale

The current study shows the potential held by mist/steam for enhancing internal steam cooling. The model herein was run at a pressure of approximately 1.1 bar, and the prototype will be operated at 30 bars. Also, the heat flux will be much higher than the values in this paper, which were nominally up to 13 kW/m^2. Table 1 summarizes the typical values of this experiment and those of the expected prototype.

The mass flow velocity is much different, resulting in an increased heat transfer coefficient by a factor of approximately 10, which, based on the analysis in [7], will reduce the effect of mist. However, the capacity of steam to carry mist will improve as the density ratio (liquid to vapor) declines. At a density ratio of 52, the steam is expected to carry much higher mist concentration than those indicated in this study. More droplets will result in higher enhancement until severe coalescence occurs. Assuming an equal value of droplet concentration in model and prototype, the increase in steam density will

Table 1
Comparison of model and prototype

Parameter	Model	Prototype
Pressure, bar	1.1	30
Saturation temperature, K	375	510
Steam density, kg/m^3	0.637	15.8
Density ratio, liq/vap	1606	51.6
Channel diameter, m	0.02	0.005
Reynolds number	15,000	350,000

be accompanied by a proportional increase in droplet number. The increased deposition velocity to the heated surface, which is very important to the heat transfer enhancement as discussed in [7], can result in an increase of about 30–40 times in particle impact rate per unit area. Therefore, the performance of mist/steam cooling in actual gas turbine application is promising.

While the current multiple-row jets can serve as a guideline to increase the impact zone for single impinging jet, further studies are required to validate the mist/steam heat transfer enhancement in high-temperature and high-pressure conditions.

4. Conclusions

This paper presents the experimental study of a mist/steam cooling system consisting of three rows of circular jet impingement in a confined channel with Reynolds numbers 7500 and 15,000, and heat fluxes ranging from 3350 to 13,400 W/m^2. The experiment results indicate that the wall temperature decreased significantly because of mist injection. A region of high cooling enhancement is observed and more extensive than those observed employing one row of circular jets or slot jet. The enhanced region of three-row jets is about $9d$ at low heat flux (3.350 kW/m^2) and about $5d$ for higher heat flux rate ($q'' = 7.54$ kW/m^2), with $m_l/m_s = \sim 3.5\%$, compared to $2d$ for single-row jets. The maximum local cooling enhancement is up to 800% by injecting 3.5% mist at low heat flux conditions and 150% for high heat wall flux conditions. The average cooling enhancement can achieve more than 100% within $2d$ distance from the stagnation line at $Re = 15{,}000$ and $m_l/m_s = 1.5\%$. The overall performance of the mist/steam cooling shows its potential for gas turbine application.

Acknowledgements

This research work was supported by the US Department of Energy under the contract number DE-FC21-92MC29061 and subcontract AGTSR 95-01-SR034. The authors would like to thank Graver Separations (Wilmington, DE) for donating the steam filters for the experiment and Mee Industries Inc. (El Monte, CA) for donating the pressure atomizers and the high-pressure pump. We appreciate the help from Dr. T. Guo in setting up the test facility.

References

[1] T. Guo, T. Wang, J.L. Gaddis, Mist/steam cooling in a heated horizontal tube, Part 1: Experimental system, ASME J. Turbomach. 122 (2000) 360–365.
[2] T. Guo, T. Wang, J.L. Gaddis, Mist/steam cooling in a heated horizontal tube, Part 2: Results and modeling, ASME J. Turbomach. 122 (2000) 366–374.
[3] T. Guo, T. Wang, J.L. Gaddis, Mist/steam cooling in a 180-degree tube, ASME J. Heat Transfer 122 (2000) 749–756.
[4] X. Li, J.L. Gaddis, T. Wang, Mist/steam heat transfer of confined slot jet impingement, ASME J. Turbomach. 123 (2001) 161–167.
[5] X. Li, J.L. Gaddis, T. Wang, Mist/steam cooling by a row of impinging jets, Int. J. Heat Mass Transfer 46 (2003) 2279–2290.
[6] X. Li, J.L. Gaddis, T. Wang, Mist/steam heat transfer with jet impingement onto a concave surface, ASME J. Heat Transfer 125 (2003) 438–446.
[7] X. Li, J.L. Gaddis, T. Wang, Modeling of heat transfer in a mist/steam impinging jet, ASME J. Heat Transfer 123 (2001) 1086–1092.
[8] M.J. Goodyer, R.M. Waterston, Mist-cooled turbines, in: Proceedings of Heat and Fluid Flow in Steam and Gas Turbine Plant, Institution of Mechanical Engineers, 1973, pp. 166–174.
[9] T. Takagi, M. Ogasawara, Some characteristics of heat and mass transfer in binary mist flow, in: Proceedings of 5th International Heat Transfer Conference, Tokyo, 1974, pp. 350–354.
[10] E.N. Ganic, W.M. Rohsenow, Dispersed flow heat transfer, Int. J. Heat Mass Transfer 20 (1977) 866–885.
[11] K. Mastanaiah, E.N. Ganic, Heat transfer in two-component dispersed flow, J. Heat Transfer 103 (1981) 300–306.
[12] H. Yoshida, K. Suenaga, R. Echigo, Turbulence structure and heat transfer of a two-dimensional impinging jet with gas–solid suspensions, Int. J. Heat Mass Transfer 33 (5) (1990) 859–867.
[13] R.J. Moffat, Using uncertainty analysis in the planning of an experiment, J. Fluids Eng. 107 (1985) 173–178.
[14] T. Wang, T.W. Simon, Development of a special-purpose test surface guided by uncertainty analysis, Int. J. Thermophys. 3 (1989) 19–26.
[15] X. Li, Cooling by a mist/steam jet, Ph.D. thesis, Clemson University, Clemson, SC, 1999.